Carlos Alberto Bavastri
Member, ABCM
bavastri@utfpr.edu.br
Univ. Tecnológica Federal do Paraná - UTFPR
80230-901 Curitiba, PR, Brazil

Euda Mara da S. Ferreira
eudaferreira@pop.com.br
Universidade Federal do Paraná - UFPR
81531-990 Curitiba, PR, Brazilç

José João de Espíndola
Life Member, ABCM
espindol@mbox1.ufsc.br
Universidade Federal de Santa Catarina – UFSC
88040-900 Florianópolis, SC, Brazil

Eduardo Márcio de O. Lopes
Senior Member, ABCM
eduardo_lopes@ufpr.br
Universidade Federal do Paraná - UFPR
81531-990 Curitiba, PR, Brazil

Modeling of Dynamic Rotors with Flexible Bearings due to the use of Viscoelastic Materials

Nowadays rotating machines produce or absorb large amounts of power in relatively small physical packages. The fact that those machines work with large density of energy and flows is associated to the high speeds of rotation of the axis, implying high inertia loads, shaft deformations, vibrations and dynamic instabilities. Viscoelastic materials are broadly employed in vibration and noise control of dynamic rotors to increase the area of stability, due to their high capacity of vibratory energy dissipation. A widespread model, used to describe the real dynamic behavior of this class of materials, is the fractional derivative model. Resorting to the finite element method it is possible to carry out the modeling of dynamic rotors with flexible bearings due to the use of viscoelastic materials. In general, the stiffness matrix is comprised of the stiffnesses of the shaft and bearings. As considered herein, this matrix is complex and frequency dependent because of the characteristics of the viscoelastic material contained in the bearings. Despite of that, a clear and simple numerical methodology is offered to calculate the modal parameters of a simple rotor mounted on viscoelastic bearings. A procedure for generating the Campbell diagram (natural frequency versus rotation frequency) is presented. It requires the embedded use of an auxiliary (internal) Campbell diagram (natural frequency versus variable frequency), in which the stiffness matrix as a frequency function is dealt with. A simplified version of that procedure, applicable to unbalance excitations, is also presented. A numerical example, for two different bearing models, is produced and discussed
***Keywords*:** *dynamic rotor, viscoelastic material, Campbell diagram, critical rotations, unbalance response*

Introduction

Nowadays rotating machines produce or absorb larger and larger amounts of power in relatively small physical packages. The fact that those machines work with large density of flows of energy is associated to the high speeds of rotor rotation. It implies high inertia loads, shaft deformations, high levels of vibrations and dynamic instabilities.

Rotating machines often have problems of instability when working at high rotations, which can result in sudden failures of the whole system or parts of it. This problem can be solved by including damping in the bearings. In general, with this type of control, not only can the vibration levels be reduced but also the area of stability can be enlarged.

Viscoelastic materials are widely employed in vibration and noise control devices due to their high capacity of vibratory energy dissipation (see Espíndola et al., 2005). In order to do so, accurate knowledge of their dynamic properties is essential.

Several works can be found in the literature, with the purpose of modeling simple rotors mounted either on viscoelastic materials or on bearings made of this type of material. Generally, those works use the Kelvin-Voigt model, as proposed by Shabaneh and Jean (1999), where the viscoelastic material is put under the bearings. This model can not accurately represent the dynamic characteristics of most viscoelastic materials used in practice, particularly when a wide frequency band is considered (Pritz, 1996; Bagley and Torvik, 1983). It is stressed that this model is described by a differential equation of integer order.

In the work accomplished by Marynowski and Kapitaniak (2002), the models of Kelvin-Voigt and Bürgers are compared in their ability of describing the behavior of a viscoelastic material.

The former is a model with two parameters (spring and viscous shock absorber in parallel) while the latter is described by four parameters. Similar results were obtained for small values of internal shock absorption, but for materials with larger coefficients of absorption the model of Bürgers proved itself more appropriate.

In Panda and Dutt (1999), polymeric materials are placed inside the bearings. Using nonlinear optimization techniques, it was possible to find the optimal dimensions to reduce the vibratory response of the system to unbalance excitations.

In Dutt and Toi (2002), models with three and four spring-shock absorber elements and integer order derivatives are used to predict the behavior of a viscoelastic material that is part of a dynamic rotor. In that paper the aim was to study the reduction of vibration and the changes in rotor dynamic behavior caused by the viscoelastic material.

In most of the papers mentioned above, the models used for describing viscoelastic materials could not reproduce their dynamic characteristics faithfully over a wide frequency band.

It will be presented herein a numerical methodology for predicting the dynamic response of a simple rotor system in steady state, with bearings containing layers of viscoelastic material. The model used for the viscoelastic material is the four parameter fractional derivative model, due to its ability of representing the real dynamic behavior of the material (Pritz, 1996). For this purpose, the characteristics of the viscoelastic material were determined by the methodology proposed in Espíndola et al. (2005) and Lopes et al. (2004).

To describe the dynamic behavior of the rotor system by Lagrange's equations, it is used the finite element method. By this way, the inertia matrix (symmetrical and with constant coefficients), the gyroscopic matrix (skew-symmetrical and a function of the rotating speed) and the complex stiffness matrix (comprised of the stiffness of the shaft and the stiffnesses of the bearings, which are frequency and temperature dependent due to the viscoelastic layers) are obtained.

A simple strategy is offered to calculate the modal parameters of the rotor system. In this strategy, a Campbell diagram is generated, through which it is possible to determine the corresponding critical rotations of the rotor system. Due to the characteristics of the system - the stiffness matrix is complex and a function of the frequency - the final Campbell diagram should be obtained through the embedded use of an auxiliary (internal) Campbell diagram.

That is, once the rotation of the shaft is established, the inertia and the gyroscopic matrices are constant, but the stiffness matrix is a function of the frequency, for a given temperature. Therefore, for each rotation, the natural frequencies of the system are frequency functions and should be found through another Campbell diagram (natural frequency versus variable frequency). These steps follow the sequence presented in Espíndola and Floody (1999), where the dynamic behavior of a sandwich beam (steel – viscoelastic material – steel) was studied.

To validate the above procedure, a numerical example on a simple rotor system will be produced and discussed at the end.

In order to make this text clearer, the classical derivations of the rotor system matrices are reviewed underneath, following very closely Lalanne's steps (see Lalanne and Ferraris, 1990). The differences related to the use of viscoelastic materials, described by the four parameter fractional derivative model, are pointed out as they appear.

Elements of the Rotor System

The rotor system being modeled is basically comprised of a shaft, one or more disks and several flexible bearings, containing layers of viscoelastic material. The force upon the rotor system can be caused by unbalanced masses (synchronous excitation, $\Omega = \Omega_{rpm}$), instabilities of hydrodynamic bearings (asynchronous excitation, $\Omega \cong 0,5\Omega_{rpm}$) or base excitation ($\Omega \neq \Omega_{rpm}$). This paper will address unbalance loads only.

The general equations of the rotor system can be derived through Lagrange's equations, seen in Eq.(1). So it is necessary to define the kinetic energy T, the potential energy U and Rayleigh's dissipation function $\wp$ of each element of the rotor system, besides the virtual work done by external forces acting upon the bearings.

$$\frac{d}{dt}\left(\frac{\partial T}{\partial \dot{q}_i}\right) - \frac{\partial T}{\partial q_i} + \frac{\partial U}{\partial q_i} + \frac{\partial \wp}{\partial \dot{q}_i} = F_{q_i} \tag{1}$$

In Eq.(1), q_i is the *ith* generalized coordinate, $\dot{q}_i$ is the *ith* generalized velocity and F_{q_i} is the *ith* generalized force. Then, using the finite element method, it is possible to describe the rotor system dynamics.

The Disk

The disk is assumed to be rigid and characterized by its kinetic energy only. Its motion is given in terms of an inertial coordinate system R_0 (X, Y, Z) and a coordinate system R (x, y, z), fixed in the center of the disk and initially coincident with R_0, as seen in Fig. 1 (Lalanne and Ferraris, 1990). The coordinates XYZ and xyz are related, in order, by three angles: ψ (rotation around the Z axis), θ (rotation around the X axis) and ϕ (rotation around the Y axis). Those angles, called the Euler angles, describe how the disk rotates as a rigid body concerning the axis X, Y or Z.

The instantaneous angular speed vector of the disk can then be written in reference system R as:

$$\bar{\omega} = \begin{bmatrix} \omega_x \\ \omega_y \\ \omega_z \end{bmatrix} \cong \begin{bmatrix} \dot{\psi}\,sen\,\phi\,cos\,\theta + \dot{\theta}\,cos\,\phi \\ -\dot{\psi}\,sen\,\theta + \dot{\phi} \\ \dot{\psi}\,cos\,\phi\,cos\,\theta - \dot{\theta}\,sen\,\phi \end{bmatrix} = \begin{bmatrix} \dot{\psi}\,sen\,\phi + \dot{\theta}\,cos\,\phi \\ -\dot{\psi}\,\theta + \Omega \\ \dot{\psi}\,cos\,\phi - \dot{\theta}\,sen\,\phi \end{bmatrix}. \tag{2}$$
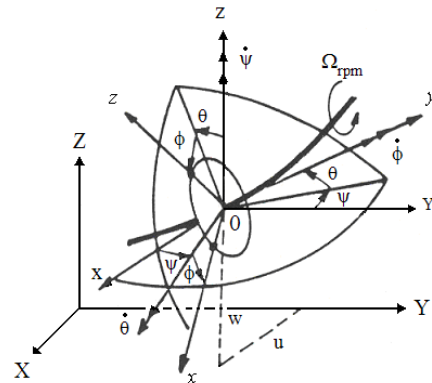

Figure 1. Coordinate systems for a disk rotating around a flexible shaft.

Assuming linearity, the angles θ (rotation around axis X) and ψ (rotation around axis Z) are regarded as small, so that $cos\,\theta \cong 1$ and $sin\,\theta \cong \theta$, the kinetic energy of the disk is then given by the equation:

$$T_D = \frac{1}{2}M_D\left(\dot{u}^2 + \dot{w}^2\right) + \frac{1}{2}\left(I_{Dx}\omega_x^2 + I_{Dy}\omega_y^2 + I_{Dz}\omega_z^2\right) \tag{3}$$

where M_D is the mass of the disk and u and w are, respectively, the displacements in the X and Z-direction (see Fig. 1). Still, in this particular case, as the disk is symmetrical, $I_{Dx}=I_{Dz}$, where I_{Dx} and I_{Dz} are the transverse inertia in the X and Z directions.

Additionally, it is assumed that the angular speed remains constant, so $\dot{\phi}=\Omega=$ constant. Therefore, the expression of the kinetic energy of the disk, neglecting the terms of second-order, is:

$$T_D \cong \frac{1}{2}M_D\left(\dot{u}^2 + \dot{w}^2\right) + \frac{1}{2}I_{Dx}\left(\dot{\theta}^2 + \dot{\psi}^2\right) + \frac{1}{2}I_{Dy}\left(\Omega^2 + 2\Omega\dot{\psi}\theta\right) \tag{4}$$

In the Eq.(4), it is observed that the term $(1/2)I_{Dy}\Omega^2$ is constant, not having any influence in Lagrange's equations. The last term, $I_{Dy}\Omega\dot{\psi}\theta$, represents the gyroscopic effect.

The Shaft

The shat is characterized by the potential and kinetic energies. The expression for the kinetic energy of the shat is the result of an extension of the kinetic energy of the disk (see Eq.(4)). If the element has length L, its kinetic energy can be expressed by the following equation:

$$T_E = \frac{\rho S}{2}\int_0^L \left(\dot{u}^2 + \dot{w}^2\right)dy + \frac{\rho I}{2}\int_0^L \left(\dot{\psi}^2 + \dot{\theta}^2\right)dy + \rho IL\Omega^2 + 2\rho I\Omega\int_0^L \dot{\psi}\theta\,dy \tag{5}$$

where I is the transverse inertia, ρ is the density and S is the transverse area.

Considering the symmetry of the axis ($I_x = I_z = I$) and neglecting the effects of axial forces, the expression for potential energy is defined by:

$$U_E = \frac{EI}{2} \int_0^L \left[\left(\frac{\partial^2 u}{\partial y^2} \right)^2 + \left(\frac{\partial^2 w}{\partial y^2} \right)^2 \right] dy \ . \qquad (6)$$

The Bearings

The bearings are comprised of two parts: the bearing itself and the viscoelastic layers. The viscoelastic layers can be added between the external layer of the roller bearing and the bearing housing or underneath the bearing housing, as shown in Fig. 2a and Fig. 2c. In the former case, the inertia of the bearing can be neglected while, in the latter, it must be considered. Figures 2b and 2d show simplified representations for both the situations mentioned above. In the current work, it was used the second alternative (Fig. 2c) only, with and without layers of viscoelastic material.

Due to the great difference in damping between the viscoelastic layers and the roller bearings, when the viscoelastic material was introduced, the damping of the roller bearing was neglected. However, when the viscoelastic material is not in place, it was considered a small amount of viscous damping, just for the response not to approach infinite at resonance.

The viscoelastic layers and the bearings are placed in series. Because of that and considering that the stiffness of the roller bearings is much higher than the stiffness of the viscoelastic layers, the resulting equivalent stiffness will be that of the viscoelastic layers.

The model used to describe the real dynamic behavior of the viscoelastic material employed in the layers is the four parameter fractional derivative model. As stated before, the use of this model in describing the dynamic behavior of rotor systems with viscoelastic bearings is a novelty.
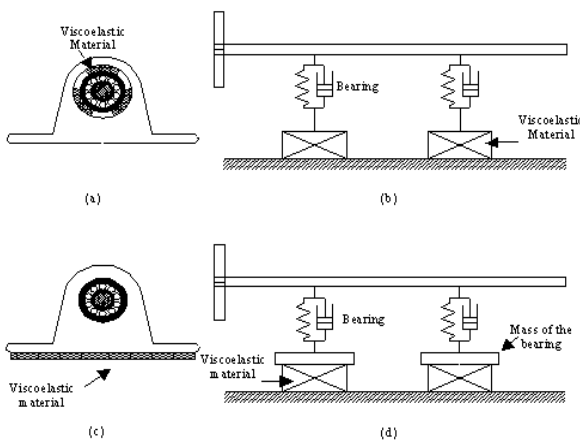

Figure 2. Models of bearings with viscoelastic material.

According to Bagley and Torvik (1983), the unidimensional constitutive equation in terms of fractional derivatives is:

$$\sigma(t) + \sum_{m=1}^M b_m D^{\beta_m} \sigma(t) = E_0 \varepsilon(t) + \sum_{n=1}^N E_n D^{\alpha_n} \varepsilon(t) \qquad (7)$$

where $\sigma(t)$ is the stress at time t, $\varepsilon(t)$ is the corresponding strain, b_m, β_m, α_n, E_0 and E_n, are the parameters for a given material. The operators D^{β_m} and D^{α_n} represent fractional derivatives.

When $M=N=1$ and $\alpha=\beta$, the above equation contains four parameters only, such that:

$$\sigma(t) + b_1 D^{\alpha} [\sigma(t)] = E_0 \varepsilon(t) + E_1 D^{\alpha} [\varepsilon(t)] \ . \qquad (8)$$

Applying the Fourier transform to both sides of Eq.(8) gives:

$$\sigma(\Omega) + b_1 (i\Omega)^{\alpha} \sigma(\Omega) = E_0 \varepsilon(\Omega) + E_1 (i\Omega)^{\alpha} \varepsilon(\Omega) \ . \qquad (9)$$

The relation $\sigma(\Omega)/\varepsilon(\Omega)$ is termed the elasticity modulus of the material, as seen in Eq.(9).

$$E_c(\Omega) = \frac{\sigma(\Omega)}{\varepsilon(\Omega)} = \left[E_0 + E_1 (i\Omega)^{\alpha} \right] / \left[1 + b_1 (i\Omega)^{\alpha} \right] \qquad (10)$$

Alternatively,

$$E_c(\Omega) = \frac{E_0 + E_\infty (i\Omega b)^{\alpha}}{1 + (i\Omega b)^{\alpha}} \qquad (11)$$

where $E_1 = E_\infty b_1$, $b_1 = b^{\alpha}$ and $E_c(\Omega)$ is the complex modulus of the material. In general, this modulus is a function of frequency and temperature. In this work, the temperature will be regarded as constant, so it will not be included as an independent variable. The elasticity modulus $E_c(\Omega)$ can be written in a general way by:

$$E_c(\Omega) = E(\Omega)(1 + i\eta(\Omega)) \qquad (12)$$

where $E(\Omega)$ is the real part of $E_c(\Omega)$, also called the dynamic modulus of elasticity, and $\eta(\Omega) = \mathrm{Im}(E_c(\Omega)) / \mathrm{Re}(E_c(\Omega))$ is the loss factor.

In Eq.(12), E_0 and E_∞ represent the lower and upper asymptotes of the dynamic modulus of elasticity. The exponent α represents the slope of a straight line, tangent to the point of inflection of the curve of $E(\Omega)$. This point corresponds to the point of maximum loss factor. The parameter b, in the same Eq.(12), is the relaxation time.

In analogy with Eq.(10), a model for the shear modulus is:

$$G_c(\Omega) = \left[G_0 + G_1 (i\Omega)^{\alpha} \right] / \left[1 + b_1 (i\Omega)^{\alpha} \right] \qquad (13)$$

or, in a general way, by

$$G_c(\Omega) = G(\Omega)(1 + i\eta(\Omega)) \qquad (14)$$

where $G(\Omega) = Re(G_c(\Omega))$ is related to the storage of vibratory and $\eta(\Omega) = \mathrm{Im}(G_c(\Omega)) / \mathrm{Re}(G_c(\Omega))$ is related to the dissipation of vibratory energy. For elastomers (Snowdon, 1968), it is known that

$$\eta(\Omega) = \eta_E(\Omega) = \eta_G(\Omega) \ . \qquad (15)$$

In the model developed herein, where the viscoelastic material is added under the bearings (see Fig. 2c), only the xx and zz components of stiffness and damping will be considered. In X direction, the stiffness will be represented by the shear modulus and in Z by the elasticity modulus.

Disregarding the stiffnesses associated to the rotations ψ and θ of the rolling bearings (in Z and X directions, respectively), the stiffness matrix of the viscoelastic layers will be given by:

$$\begin{bmatrix} F_u \\ F_w \end{bmatrix} = - \begin{bmatrix} \bar{k}_{xx} & 0 \\ 0 & \bar{k}_{zz} \end{bmatrix} \begin{bmatrix} u \\ w \end{bmatrix} \qquad (16)$$

where

$$\bar{k}_{xx} = L G_c(\Omega) \qquad (17)$$

and

$$\bar{k}_{zz} = L E_a(\Omega) = L E_a(\Omega) . \qquad (18)$$

In the Eq.(18), A is the loaded area, h is the viscoelastic layer thickness, $L = A/h$ and E_a is the apparent modulus of elasticity, given by (Nashif et al, 1985)

$$E_a = k_T E_c \qquad (19)$$

which means that the apparent modulus of elasticity is obtained by the shape factor k_T times the complex modulus of elasticity. In this paper, the layer of viscoelastic material is conceived in a such way (see Fig. 3) that lateral expansion is allowed, so that k_T tends to 1 and E_a tends to E_c.

In the transition frequency of elastomers, it can be regarded that Poisson's coefficient is approximately equal to 0,5 (Snowdon, 1968 and Nashif et al, 1985), so that $E_a = 3G_c$. Then, Eq.(18) takes the following form:

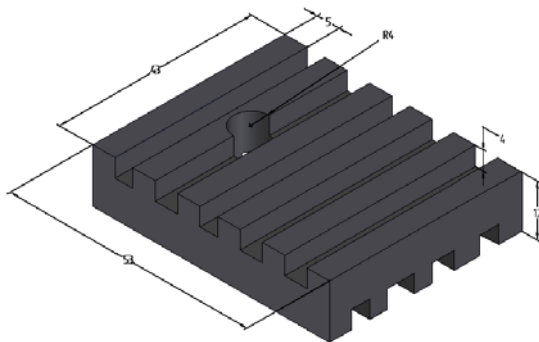$$\bar{k}_{zz} = 3 L G_c(\Omega) . \qquad (20)$$

Figure 3. Shape of the layer of viscoelastic material.

Matrix Representation of the Rotor

In line with the classical developments (Lalanne and Ferraris, 1990), it is considered that each element node of the shaft has four degrees of freedom: two displacements u and w (in X and Z directions, respectively) and two rotations θ and ψ (around the axes X and Z, respectively). Therefore, for node i, the generalized coordinate q_i is represented by:

$$q_i = \begin{bmatrix} u_i, w_i, \theta_i, \psi_i \end{bmatrix}^T . \qquad (21)$$

By now applying Lagrange's equations to the kinetic and potential energies of the elements of a simple rotor system and assembling each elementary matrix conveniently, including stiffness matrix of viscoelastic material (Eq.(19)), the following algebraic equations in the frequency domain result (Espíndola and Bavastri, 1997):

$$\left[-\Omega^2 M + i\Omega\, G(\Omega_{rpm}) + \bar{K}(\Omega) \right] Q(\Omega) = F(\Omega) \qquad (22)$$

where

M is the inertia matrix (constant and symmetrical);

G is the gyroscopic matrix of the shaft and disk (function of rotation and skew-symmetric);

$\bar{K}(\Omega)$ is the stiffness matrix for the dynamic rotor system with viscoelastic bearings (symmetric, complex and frequency-temperature dependent). Note that the overall viscous damping matrix is zero here and the temperature is regarded as constant, as explained previously;

$F(\Omega)$ is the Fourier transform of the time domain excitation;

$X(\Omega)$ is the Fourier transform of the time domain response.

Given the approach adopted herein, the complex stiffness of each viscoelastic layer is defined by:

$$\bar{K}(\Omega)_m = \begin{bmatrix} LG(\Omega)[1 + i\eta(\Omega)] & 0 & 0 & 0 \\ 0 & 3LG(\Omega)[1 + i\eta(\Omega)] & 0 & 0 \\ 0 & 0 & 0 & 0 \\ 0 & 0 & 0 & 0 \end{bmatrix} . \qquad (23)$$

Matrices as expressed by Eq.(23) will be inserted into the global stiffness matrix $\bar{K}(\Omega)$ at the places corresponding to the positions of the bearings in the rotor system.

Solution of the System of Dynamic Equations

The system of equations that represents the motion of a dynamic rotor system in the frequency domain is given by Eq.(22). This set of equations is dependent on the excitation frequency, Ω, when the rotation of the shaft, Ω_{rpm}, is fixed.

The Complex Eigenvalue Problem

To solve the resulting complex eigenvalue problem, a transformation of the generalized coordinates to the state space (Ewins, 1984; Espíndola and Bavastri, 1997) is carried out. Then, a new $2n$ x 1 vector of coordinates $Y(\Omega)$ is defined as

$$Y(\Omega) = \begin{Bmatrix} Q(\Omega) \\ \cdots \\ i\Omega\, Q(\Omega) \end{Bmatrix} . \qquad (24)$$

To represent the system of equations in the state space, it is also considered the following equality:

$$i\Omega M\, Q(\Omega) - i\Omega M\, Q(\Omega) = 0 \qquad (25)$$

which results in

$$\left[i\Omega A(\Omega_{rpm}) + B(\Omega) \right] Y(\Omega) = \{ F_y(\Omega) \} \qquad (26)$$

where

$$A(\Omega_{rpm}) = \begin{bmatrix} G(\Omega_{rpm}) & \vdots & M \\ \cdots & \vdots & \cdots \\ M & \vdots & 0 \end{bmatrix}_{2nx2n} , \quad B(\Omega) = \begin{bmatrix} \bar{K}(\Omega) & \vdots & 0 \\ \cdots & \vdots & \cdots \\ 0 & \vdots & -M \end{bmatrix}_{2nx2n}$$

and $\left\{ F_y\left(\Omega\right) \right\} = \begin{Bmatrix} F\left(\Omega\right) \\ \ldots \\ 0 \end{Bmatrix}_{2nx1}$.

If Ω_{rpm} is fixed, it is possible to assemble the following eigenvalue problem:

$$\lambda_j\left(\Omega\right) A\, \theta_j\left(\Omega\right) = B\left(\Omega\right)\theta_j\left(\Omega\right) \tag{27}$$

where λ_j is the jth eigenvalue and θ_j is the jth right eigenvector, with $j = 1$ to $2n$.

Considering that A and/or B are not symmetrical matrices, the adjoint problem of eigenvalues must also be solved, which is:

$$B\left(\Omega\right)^T \varphi_j\left(\Omega\right) = \lambda_j\left(\Omega\right) A^T \varphi_j\left(\Omega\right) \tag{28}$$

where φ_j is the jth left eigenvector, with $j = 1$ to $2n$.

Orthogonality

It is known (Espíndola and Bavastri, 1997) that the following relations, for a given pair Ω and Ω_{rpm}, are satisfied:

$$\varphi_j^T A\ \theta_k = a_j\delta_{jk} \tag{29}$$

$$\varphi_j^T B\ \theta_k = b_j\delta_{jk} \tag{30}$$

where δ_{ik} is the Kroneker delta. From Eq.(29) and Eq.(30), the following orthogonality properties in the state space are obtained

$$-\lambda_j\lambda_k\varphi_j^T M\, \theta_K + \varphi_j^T \overline{K}\theta_K = b_j\delta_{jk} \tag{31}$$

$$-(\lambda_j + \lambda_k)\varphi_j^T M\, \theta_K + \varphi_j^T G\left(\Omega_{rpm}\right)\theta_K = a_j\delta_{jk} \;. \tag{32}$$

Equations (31) and (32) represent the orthogonality conditions as functions of matrices M, G and K. As the values of λ are complex, they can be represented by their real parts, δ_j, and their imaginary parts, υ_j, as

$$\lambda_j = \delta_j + i\upsilon_j \;. \tag{33}$$

Although the eigenvalues are complex and different, they are related, once they are obtained in the state space. In fact, it is verified that the eigenvalues are formed by pairs λ_j and $-\lambda_j$. Therefore, taking values of $j \neq k$, but with $\lambda_j = -\lambda_k$, and applying these values in the orthogonality relationships above, the result is:

$$\lambda_j^2 = -\frac{\overline{k}_j}{m_j} \;. \tag{34}$$

By definition,

$$-\lambda_j^2 = \Omega_j^2\left(1 + i\eta_j\right) \tag{35}$$

so that

$$\Omega_j^2\left(1 + i\eta_j\right) = -\lambda_j^2 = -\left(-\frac{\overline{k}_j}{m_j}\right) \tag{36}$$

where $\Omega_j^2 = \mathrm{Re}\left(-\lambda_j^2\right)$ and the loss factor is $\eta_j = \mathrm{Im}\left(-\lambda_j^2\right)/\mathrm{Re}\left(-\lambda_j^2\right)$. Note that the natural frequency Ω_j, for $j=1$ to n, is not necessarily equal to the undamped natural frequency (Ewins, 1984).

Final and Auxiliary Campbell Diagrams

For the current case, where the rotor system is mounted on bearings with viscoelastic material, matrix A, which contains the gyroscopic matrix, is a function of the rotation of the shaft, Ω_{rpm}, and matrix B is complex and a function of the frequency Ω. So, the eigenvalue problem is a function of the rotation and the frequency. That is, for a given rotation of the rotor (Ω_{rpm} = cte), the eigenvalue problem is a function of the frequency and will be solved by the embedded use of an auxiliary (internal) Campbell diagram, traced for Ω_j x Ω, because $\overline{K}(\Omega) = K(\Omega)\left(1 + i\eta\left(\Omega\right)\right)$.

Starting from this auxiliary Campbell diagram, considering $\Omega = \Omega_j$ and using a straight line that crosses the curves of the natural frequencies, the natural frequencies of the system are extracted in an equivalent way to Espíndola and Floody (1999). This process should be repeated for all the rotor rotations, resulting then in the final (external) Campbell diagram, traced now for Ω_j x Ω_{rpm}, which contains the critical rotations of the viscoelastic dynamic rotor system. From this final Campbell diagram, it is possible to determine the dynamic characteristics of the viscoelastic rotor system.

Figure 4 shows an outline of how the Campbell diagrams are built. Figure 4b represents the auxiliary (internal) Campbell diagram and Fig. 4a the final (external) Campbell diagram. As can be observed, to calculate the natural frequencies of the system for a constant rotation, it is necessary to solve a frequency dependent eigenvalue problem, given the characteristics of the stiffness matrix.
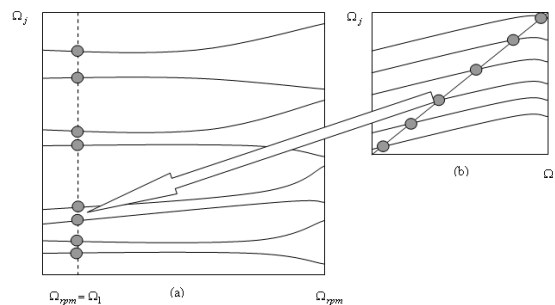

Figure 4. a) Final Campbell diagram. b) Auxiliary Campbell diagram.

For the adjoint eigenvalue problem, it is necessary to consider that A and/or B are non-symmetrical. A schematic diagram that shows how both the eigenvalue and the adjoint eigenvalue problems should be solved for a rotating system with viscoelastic bearings is given by

$$\begin{bmatrix} \begin{array}{l} Rotation\ \ loop\ (\Omega_{rpm}) \\ \begin{bmatrix} Frequency\ \ loop\ (\Omega) \\ B\theta = \lambda\,A\theta \\ B^T\psi = \lambda\,A^T\psi \\ Auxiliary\ Campbell\ diagram \end{bmatrix} \\ Final\ Campbell\ diagram. \end{array} \end{bmatrix}$$

Simplified Campbell Diagram

If unbalance excitation is considered, the above procedure can be simplified (see Espíndola and Bavastri, 1997). In this case, frequency and rotation are the same ($\Omega_{rpm} = \Omega$) and the gyroscopic matrix is such that $G(\Omega_{rpm}) = G(\Omega) = \Omega G_1$. Then, from Eq.(22), it is possible to obtain:

$$\left[-\Omega^2 M + i\Omega \left(\Omega G_1 \right) + \overline{K}(\Omega) \right] Q(\Omega) = F(\Omega) \tag{37}$$

or

$$\left[-\Omega^2 \hat{M} + \overline{K}(\Omega) \right] Q(\Omega) = F(\Omega) \tag{38}$$

where $\hat{M} = M - iG_1$.

Since $\hat{M}$ is not a symmetric matrix, the right and left eigenvalue problems must be calculated, as shown in Eqs.(42) and (43):

$$\overline{K}(\Omega) \phi_j(\Omega) = \lambda_j(\Omega) \, \hat{M} \, \phi_j(\Omega) \tag{39}$$

and

$$\overline{K}(\Omega)^T \psi_j(\Omega) = \lambda_j(\Omega) \, \hat{M}^T \, \psi_j(\Omega). \tag{40}$$

As can be seen in Eq.(38), there is only one variable, $\Omega_{rpm} = \Omega$. As the stiffness matrix is frequency dependent, both the eigenvalue problems must be solved for each frequency, Ω.

The resulting simplified Campbell diagram, traced for $\Omega_j \; x \; \Omega$, is used to represent the shaft-rotor system characteristics when only unbalance excitation is considered. A 45 degree straight line in that simplified diagram, which is, in fact, the final diagram, makes it possible to obtain the critical rotations for this kind of problem. That is similar to the single step of Fig. 4b.

Unbalance Excitation and Frequency Response

Considering Eq.(38), the response of the rotor system in the frequency domain is obtained by the following transformation:

$$Q(\Omega) = \Phi(\Omega) \, P(\Omega) \tag{41}$$

where $\Phi(\Omega)$ is the right eigenvectors matrix.

Taking Eq.(41) into Eq.(38) and pre-multiplying by $\Psi(\Omega)^T$, where $\Psi(\Omega)$ is the left eigenvector matrix and both $\Psi(\Omega)$ and $\Phi(\Omega)$ are orthonormalized by the mass matrix $\hat{M}$, it results that:

$$\Psi^T(\Omega) \left[-\Omega^2 \hat{M} + \overline{K}(\Omega) \right] \Phi(\Omega) P(\Omega) = \Psi^T(\Omega) F(\Omega) \tag{42}$$

or

$$\left[-\Omega^2 I + \Lambda(\Omega) \right] P(\Omega) = \Psi^T(\Omega) F(\Omega) \tag{43}$$

where I is the identity matrix, $\Lambda(\Omega) = \Psi^T(\Omega) \overline{K}(\Omega) \Phi(\Omega)$ and $P(\Omega)$ is the modal space response, also called principal generalized coordinates. These coordinates can thus be defined by:

$$P(\Omega) = \left[-\Omega^2 I + \Lambda(\Omega) \right]^{-1} \Psi^T(\Omega) F(\Omega) \, . \tag{44}$$

By replacing Eq.(44) into Eq.(41), the response of the system, in the frequency domain, is:

$$Q(\Omega) = \Phi(\Omega) \left[-\Omega^2 I + \Lambda(\Omega) \right]^{-1} \Psi^T(\Omega) F(\Omega). \tag{45}$$

Numerical Example

The preceding developments were applied to run a numerical example of a simple dynamic rotor system with two disks (one larger than the other), mounted on roller bearings and viscoelastic layers, as showed in Fig. 5a. A detail of the viscoelastic layers under a roller bearing is showed in Fig. 5b. The physical characteristics of the rotor system are presented in Table 1.
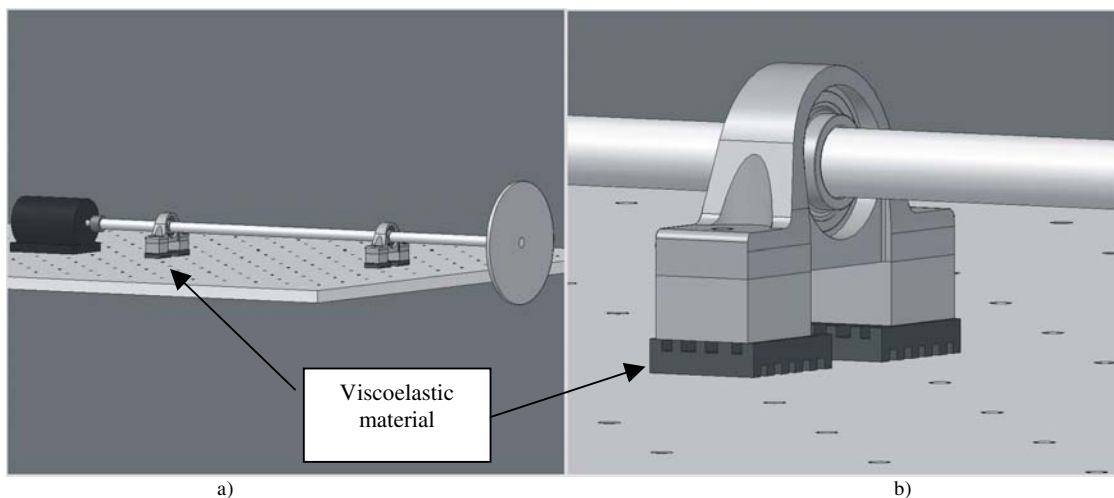

Viscoelastic material

a)   b)

Figure 5. a) Schema of the rotor system; b) Detail of a roller bearing with viscoelastic layers.

Table 1. Rotor system data.

Shaft data:	Disk data:
Total length, L = 1.05 m;	Number of disks, ND = 2;
Diameter, d = 0.025 m;	External radius, Rext = [0.140, 0.0222] m;
Elasticity modulus, E=210x10^9 MPa;	Internal radius, Rint = [d/2, d/2] m;
Poisson coefficient, ν = 0.3;	Thickness, h = [0.01, 0.035] m;
Density, ρ= 7800 Kg/m^3.	Position, pd = [0.0, 0.0275] m;
	Density, ρ = [7800, 7800] Kg/m^3.
Bearing data:	
Stiffness, Eq. (17);	Viscoelastic material data:
Number of bearings, NB = 2;	Shear modulus and loss factor, Eqs.(15)
Position, pb = [0.1835, 0.6435] m;	and (16), respectively, and "Fig. 6".
Mass, Mb = [0.770, 0.770] kg;	
Moment of Inertia, Ibxx = [0.00159018,	Unbalance excitation:
0.00159018]	Unbalanced mass, m = 0.005 kg;
Moment of Inertia, Ibzz = [0.00690495,	Eccentricity, e = 5.0x10^{-5} m;
0.00690495]	

The dynamic characteristics of the viscoelastic material, pure butyl rubber, were previously determined in the Laboratory of Vibrations and Acoustics of the Federal University of Santa Catarina (PISA/LVA/UFSC). A four parameter fractional derivative model was used to dynamically characterize the behavior of that viscoelastic material. The corresponding parameters, for reference temperature T_0=273.0 K and environmental temperature T=293.0 K, were: $G_0 = 1.53 \times 10^6$ Pa, $G_1 = 1.49 \times 10^6$ Pa, $\alpha = 0.396$ and $b_1 = 1.34 \times 10^{-2}$. Figure 6 shows the dynamic shear modulus and the associated loss factor as functions of both frequency and temperature.

Figure 7 shows the finite element model used in the current numerical example. The shaft was modelled by Timoshenko beam elements with a C_1 class interpolation function. There were fifteen elements with four degrees of freedom in each node. The two roller bearings, which could or not have viscoelastic layers underneath, were located at the fourth and tenth nodes. The two disks were placed at the first node, as showed in Fig. 7, since they were comprised, in fact, of a larger disk and short sleeve, used for attaching the former tightly to the shaft.

determines, amongst all the natural frequencies of the system, those taking part in the response to the unbalance excitation. These frequencies are known as the critical rotations of the rotor system.
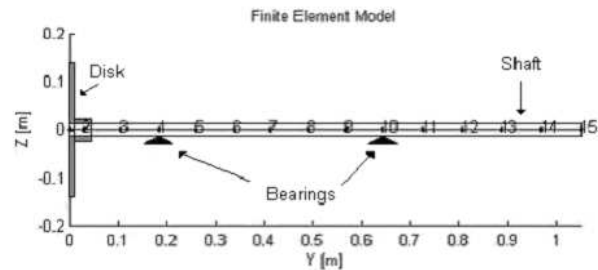

Figure 7. Finite element model.

It is highlighted that the proposed methodology allows the determination of the dynamic characteristics of the rotor system when its stiffness matrix varies with frequency. This dependence on frequency is due to the presence of the viscoelastic layers under the bearings
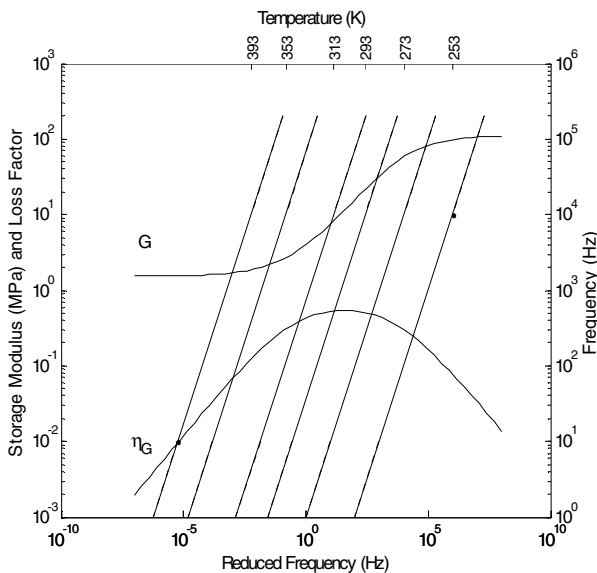

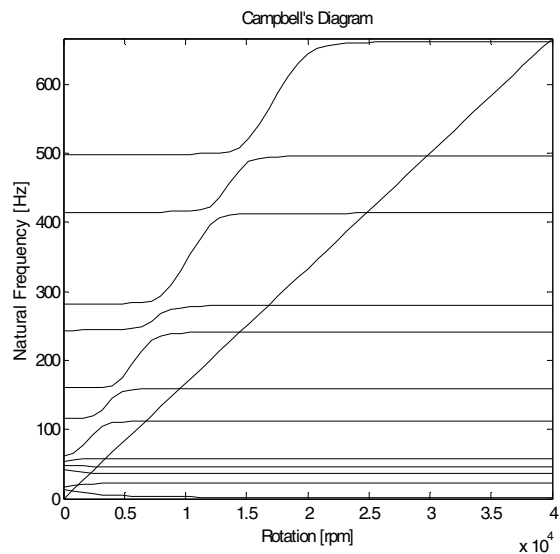**Figure 6. Dynamic properties – Pure butyl rubber.**

The results will be initially presented for the case in which the viscoelastic layers were under the bearings. Thus, Fig. 8 shows the simplified Campbell diagram and the straight line Ω_1 which

Figure 8. Simplified (final) Campbell diagram.

Figure 9 depicts the frequency domain response due to the unbalance excitation specified in Table 1. This response (which is not a frequency response function, but a response in the frequency domain) is about x-axes, at node 1 of the finite element model. The rotor system is considered as still attached to the ground through viscoelastic layers (as seen in Fig. 5b). Due to the characteristics of these layers, the rotor system is not symmetric. Therefore, an unbalance excitation can cause both the forward and backward whirls, which can be inferred from the same Fig. 9 by the amount of observed resonance peaks.

In Fig. 10, it is shown the response of a rotor system with similar characteristics of that of Table 1, except for the fact that, now, the bearings are simply ball-bearings, without viscoelastic layers underneath. The stiffness values are 1.0×10^9 N/m, in both directions, and there is also an equivalent viscous damping equal to 100 Ns/m. In this case, the dynamic rotor system is symmetric and the response presents the forward whirl only.

Comparing Fig. 9, for the case in which viscoelastic layers were under the roller bearings, and Fig. 10, for the case in which they were not, it is observed that the *X*-direction amplitude is much higher in Fig. 10 than in Fig. 9.
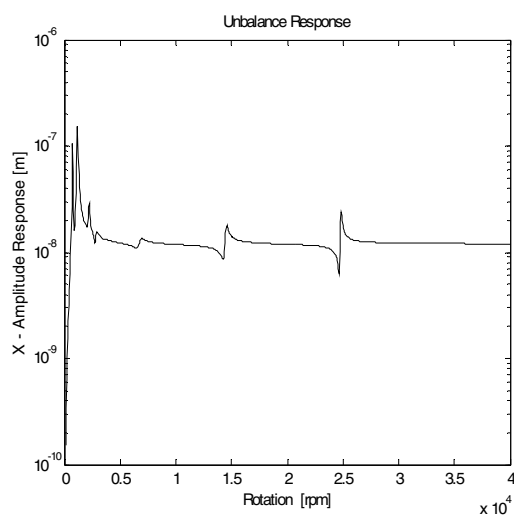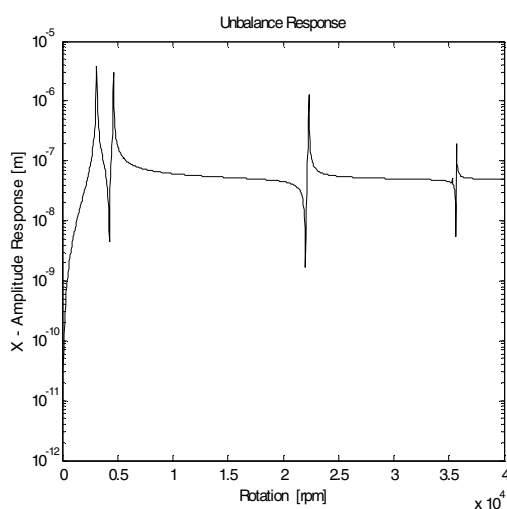
Conclusions

It was presented a simple, novel and accurate methodology to determine the final Campbell diagram of a dynamic rotor system with bearings contaning viscoelastic layers. Unlike previous works, the viscoelastic material employed in the bearings was represented with the aid of the four parameter fractional derivative model, which is proved to faithfully describe the dynamic characteristics of this class of materials.

Due to the characteristics of the stiffness matrix of this system, which is frequency dependent, it was required, in fact, to assemble two Campbell diagrams, one inside the other, in order to raise the overall dynamic behavior of the rotor system. A simplified procedure could be established for the case of unbalance excitation.

A numerical example was run in order to apply and validate the simplified procedure. Apart from achieving that aim, it was also shown that the use of viscoelastic materials in the bearings can be very efficacious in vibration and noise control.

It is therefore believed that the methodology introduced by this work is of foremost importance in guiding vibration and noise control actions on rotor systems by the use of viscoelastic materials.

Acknowledgements

References

Bagley, R.L. and Torvik, P.J., 1983, "A Theoretical Basis for the Application of Fractional Calculus to Viscoelasticity", Journal of Rheology, Vol. 27 (3), pp. 201-210.

Dutt, J.K. and Toi, T., 2002, "Rotor Vibration Reduction With Polymeric Sectors", Journal of Sound and Vibration, Vol. 262, pp. 769-793.

Espíndola, J.J., Silva Neto, J.M. and Lopes, E. M. O., 2005, "A Generalized Fractional Derivative Approach to Viscoelastic Material Properties Measurement", Applied Mathematics and Computation, Vol. 164(2), pp. 493-506.

Espíndola, J.J. and Bavastri, 1997, "An Efficient Concept of Transmissibility for a General Equipment Isolation System". In: DETC'97/VIB-4120, Sacramento, California. ASME Design Engineering Technical Conferences, v. CD ROM. p. CD-CD.

Espíndola, J.J. and Floody, S. E., 1999, "On the Modeling of Metal-Elastomer Composite Structures: A Finite Element Method Approach", Applied Mechanics in the Americas - PACAM IV, Vol. 8, pp.1335-1342.

Ewins, D.J., 1984, "Modal Testing Theory and Practice". Research Studies Press, England.

Lalanne, M. and Ferraris, G., 1990, "Rotordynamics Prediction in Engineering", John Wiley & Sons, New York, USA.

Lopes, E.M.O., Bavastri, C.A., Silva Neto, J.M., e Espíndola, J.J., 2004, "Caracterização Dinâmica Integrada de Elastômeros por Derivadas Generalizadas", Anais do III CONEM, Belém, Brasil (cd-rom, artigo 56076).

Marynowski, K. and Kapitaniak, T., 2002, "Kelvin-Voigt versus Bürgers Internal Damping in Modeling of Axially Moving Viscoelastic Web", International Journal of Non-Linear Mechanics, Vol. 37, pp. 1147-1161.

Nashif, A.D., Jones, D.I.G. and Henderson, J.P., 1985, "Vibration Damping", John Wiley & Sons.

Panda, K.C. and Dutt, J.K., 1999, "Design of Optimum Support Parameters for Minimum Rotor Response and Maximum Stability Limit", Journal of Sound and Vibration, 223 (1), pp.1-21.

Pritz, T., 1996, "Analysis of Four-Parameter Fractional Derivate Model of Real Solid Materials". Journal of Sound and Vibration, Vol. 195, pp. 103-115.

Shabaneh, N.H. and Jean W., 1999, "Dynamic Analysis of Rotor-Shaft Systems with Viscoelastically Supported Bearings", Mechanism and Machine Theory, University of Toronto, Canada.

Snowdon, J.C., 1968, "Vibration and Shock in Damped Mechanical Systems", John Wiley & Sons, New York, USA.

Figure 9. Response of the rotor system with viscoelastic bearings.

Figure 10. Response of the rotor system with ball bearings.